Journal of Engineering and Applied Sciences 14 (16): 5955-5961, 2019
ISSN: 1816-949X

GUI-based Autofocusing System for AOI of FPDs

Bonghwan Kim, Dongsu Lee, Sun Lu and Kyunghan Chun
School of Electronic and Electrical Engineering, Daegu Catholic University,
38430 Gyeongbuk, Korea

Abstract: In the Flat Panel Display (FPD) industry, Automatic Optical Inspection (AOI) is one of the most essential processes for inspection of Liquid Crystal Display (LCD) panels. For this purpose, autofocusing is an important function for which precise moving distance control in μm is required, considering the unit of focal length of autofocusing equipment. A Z-axis test bench using a step motor was built for autofocusing of the AOI camera and the moving distance was controlled by a Micro Controller Unit (MCU). A user-friendly Graphic User Interface (GUI) platform was implemented as the supervising system. The validation test confirmed the controllable minimum moving distance and verified the equipment reliability through iterative experiments. The test results can also be used to find the appropriate application range.

Key words: Autofocus, AOI, LCD, ACF, Z-axis, GUI

INTRODUCTION

Chung *et al*. (2010) reports that there has recently been an increasing requirement for high-precision Automatic Optical Inspection (AOI) systems for equipment such as Liquid Crystal Display (LCDs) panels, Plasma Display Panels (PDPs) and Organic Light Emitting Diodes (OLEDs). As the next generation technology in the area of inspection platforms, precision positioning and transfer flatness control within 10 μm are required for inline processes such as AOI. The requirements of the high-precision linear inspection module are maximum positioning accuracy and notable transfer flatness. Extensive research has been conducted on AOI (Chung *et al*., 2010; Yubao, 2013; Martinez *et al*., 2013; Dong *et al*., 2014; Tao *et al*., 2014; Jing *et al*., 2015; Kim *et al*., 2017; Lee *et al*., 2018; Sunlu *et al*., 2018). Anisotropic Conductive Films (ACFs) are popular in the assembly of electronic devices. To verify the bonding of ACFs, a microscopic indentation mark is used. As one of the quantitative methods for Differential Interference Contrast (DIC) calibration and ACF image verification, consistent calibration of DIC was investigated and quantized image verification was suggested by Kim *et al*. (2017). Artificial light is one of the major components of the general AOI system. There are various sources such as halogen, xenon and LED lamps. The relationship between the DIC microscope and these sources was investigated and recommendations were made by Lee *et al*. (2018) based on the comparison of test results. The image acquisition device is another important component of the AOI system with many parameters that control the inspection image. Image processing system parameters were analyzed by Chun *et al*. (2018) to enhance inspection performance and test images were compared to improve inspection results.

In this study, we propose a Graphic User Interface (GUI)-based autofocusing AOI system for Flat Panel Displays (FPDs). The system is composed of three parts, namely a Z-axis test bench, Micro Controller Unit (MCU) for the test bench motor and GUI-based supervising software implemented on a Personal Computer (PC). The Z-axis test bench has been designed and prototyped to control transfer flatness in the micrometer range. The MCU controls the step motor in the test bench and communicates with the supervising software to receive commands and send measured sensor values. The whole system has been developed and tested to verify its performance.

MATERIALS AND METHODS

ATF system

Principle of autofocusing: The general structure of the Autofocus and Tracking (ATF) system for vision inspection is composed of an optical lens including an objective lens, a camera, a sensor for sensing the displacement of the test surface, a controller for calculating a sensed displacement amount and a Z-driver that moves the objective lens as shown in Fig. 1.

The operating principle of the ATF system is that the ATF sensor (usually laser diode or Infra-Red (IR)) detects the displacement of the inspection region on the same axis

Corresponding Author: Kyunghan Chun, Daegu Catholic University, 38430 Gyeongbuk, Korea, kchun@cu.ac.kr

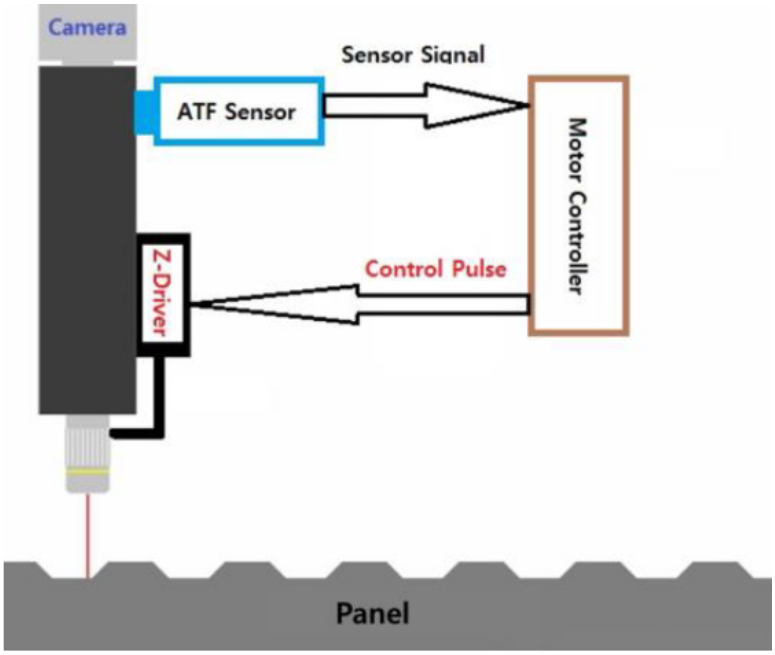

Fig. 1: Autofocusing mechanism

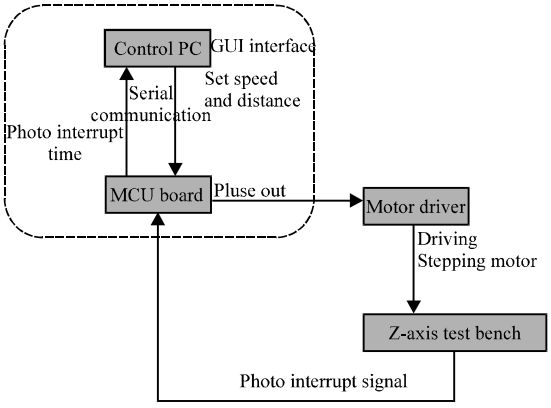

Fig. 2: Z-axis test bench flow diagram

in real time and sends it to the ATF controller. The measured value is compared with the initial setting value (the value used by the inspector who manages the ATF to focus it manually) and this determines whether to move the objective lens. The motor driver controls the stepping motor which is mechanically connected to the objective lens. The pulse value corresponding to the displacement amount is transmitted and the motor driver starts the stepping motor.

Autofocusing system: The test bench flow diagram is shown in Fig. 2. The MCU control program which drives the stepping motor was coded in C. The PC GUI program which is the interface between the MCU board and PC controller was coded in C# and RS-232C serial communication is applied for communication between the PC controller and MCU.

When the stepping motor speed and target point have been set and transferred to the MCU by the PC controller, the MCU commands the motor driver to rotate the step motor. For the speed test, the photo interrupter sensors are mounted on the Z-axis driver test bench and the output is sent to the MCU; the control PC receives the signal from the MCU and calculates the driving speed of the Z-axis test bench. In order to test the control parameters of the Z-axis driver, a Z-axis test bench was designed as shown in Fig. 3.

Z-axis autofocusing mechanism: To comprehend the mechanism of the Z-axis driver, panel moving speed and line scan camera, it is first necessary to understand the kinematic relationship between the optical system including the objective lens and line scan camera and the inspection panel in the LCD as shown in Fig. 4. Next, we calculate the time needed for shooting an image. The inspection panel moves at 40 mm/sec. Therefore, the time needed to move one pixel distance (0.7 μm) is as follows:

$$\begin{aligned} \text{Time} &= \text{Moving distance/speed} \\ &= (0.7\ \mu\text{m}/1000)/40\ \text{mm/sec} \\ &= 0.0000175\ \text{sec} = 0.0175\ \text{msec} \\ &= 17.5\ \mu\text{sec} \end{aligned} \quad (1)$$

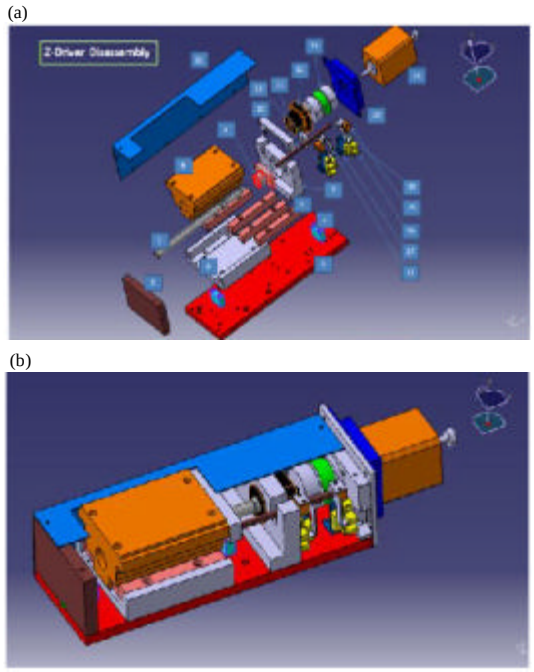

Fig. 3: Z-axis test bench: a) Before assembly and b) After assembly

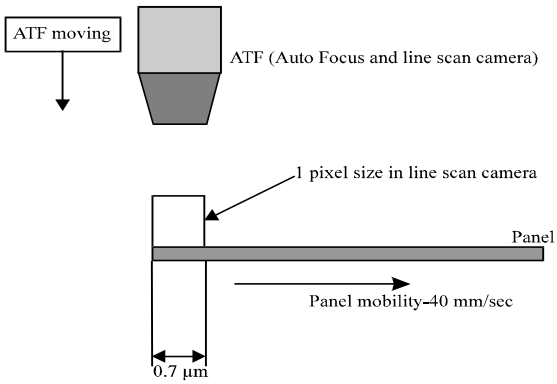

Fig. 4: Line scanning with autofocus for moving panel

That is the exposure and shutter time required by the line scan camera to shoot one pixel size (0.7 µm) should be 17.5 µsec or less. Exposure and shutter time of line scan cameras currently distributed in the market is less than 17.5 µsec. Even for a much shorter range than the above-calculated value, a line scan camera can be applied.

GUI-based control software: The PC controller software was designed to conveniently control the parameters of the objective lens through the GUI during auto focusing. Although, it was originally designed to test the Z-axis driver, the basic program structure has the functionality to fine-tune the focus of the inspection panel during autofocusing. At present, a function has not been implemented to adjust the objective lens by receiving the measured displacement value. However, it can be programmed to adjust the objective lens automatically by receiving the sensing value from the displacement sensor via the current communication protocol. A brief description follows of the software's GUI menu as shown in Fig. 5. The GUI window consists of four sections, namely "Connection", "Setting Motor", "Control" and "Focus Speed Test".

Connection: This menu specifies the communication port and baud rate for communication with the MCU. By clicking the "Connect" button, serial communication with the MCU commences.

Setting motor: The stepping motor rotates at a speed proportional to the frequency of the pulse signal. The input unit for speed is Hz. The larger the input value, the faster the rotation speed of the stepping motor. The stepping motor maintains its current speed until the input value is changed.

Control: This menu is used to set the target point by specifying the number of pulses to rotate the stepping motor. The basic step angle of the stepping motor (PKP246U12B-L, two-phase) used in this study is 1.8° where step angle is the angle at which the motor shaft rotates relative to a single pulse. Thus, the input pulse required for one rotation of the motor is:

$$\text{Pulse/rev} = 360°/1.8° = 200 \text{ steps} \quad (2)$$

For example, if you enter 2000 steps the stepping motor shaft rotates 10 times. The "Forward" and "Backward" buttons on the menu set the stepping motor direction of movement as Clockwise (CW) and counter Clockwise (CCW), respectively. The "<<" and ">>" buttons advance the stepping motor 10 steps at a time.

Focus speed test: This menu is for the stepping motor speed test. To measure the speed two sensors are located 5 mm apart on the test bench as shown in Fig. 6. During speed testing, the slider touches sensor 1 which switches off the sensor. The slider continues to move until it touches sensor 2. When sensor 2 is switched off, the stepping motor automatically stops and the time difference is recorded in the "Time" textboxes. The linear motion speed is then calculated as follows:

$$\text{Speed} = 5\text{m}/\text{Time difference} \quad (3)$$

RESULTS AND DISCUSSION

Test and validation: The implementation of the GUI-based autofocusing test bench is shown in Fig. 7. The step

Fig. 5: Z-axis test bench GUI

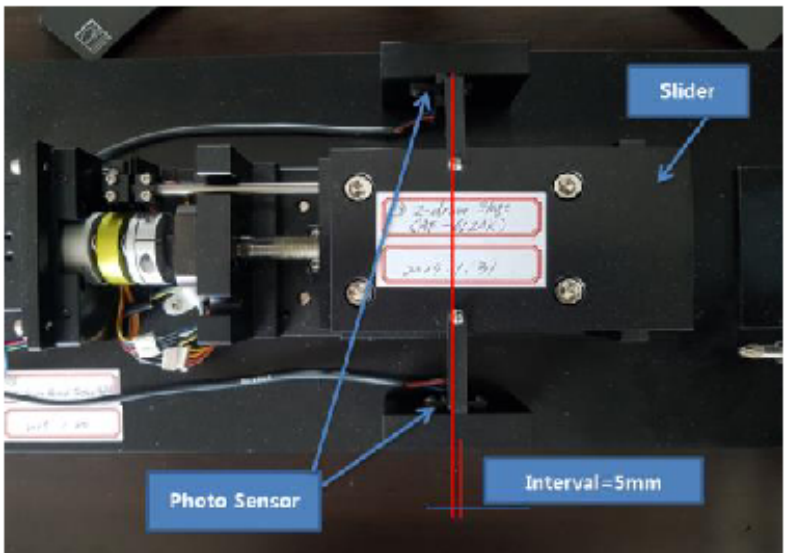

Fig. 6: Speed test sensors

angle can be changed according to the mode; the step angle becomes smaller with an increasing resolution. It is calculated by Eq. 4 and the results of the step angle for given resolutions are shown in Table 1).

$$\text{Step angle} = 360°/\text{Resolution} \quad (4)$$

The motor driver has two pulse input methods, namely a two-pulse (CW/CCW) method and a one-pulse

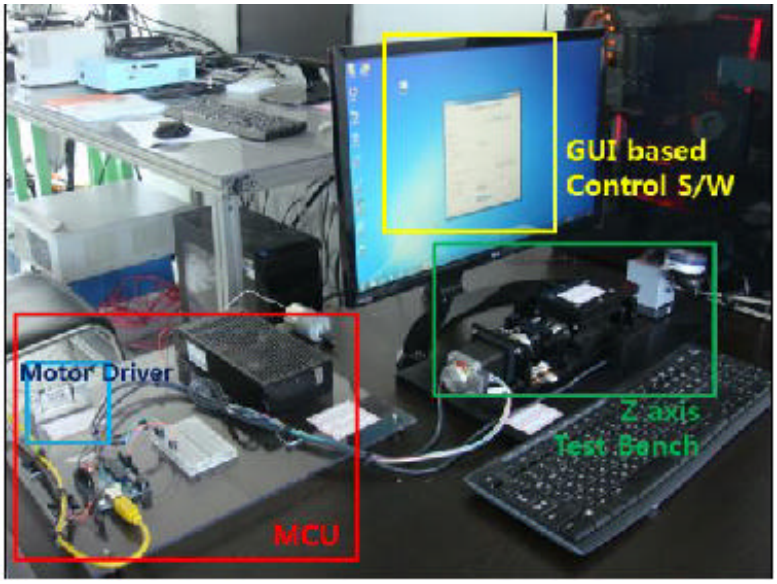

Fig. 7: GUI based autofocusing test bench

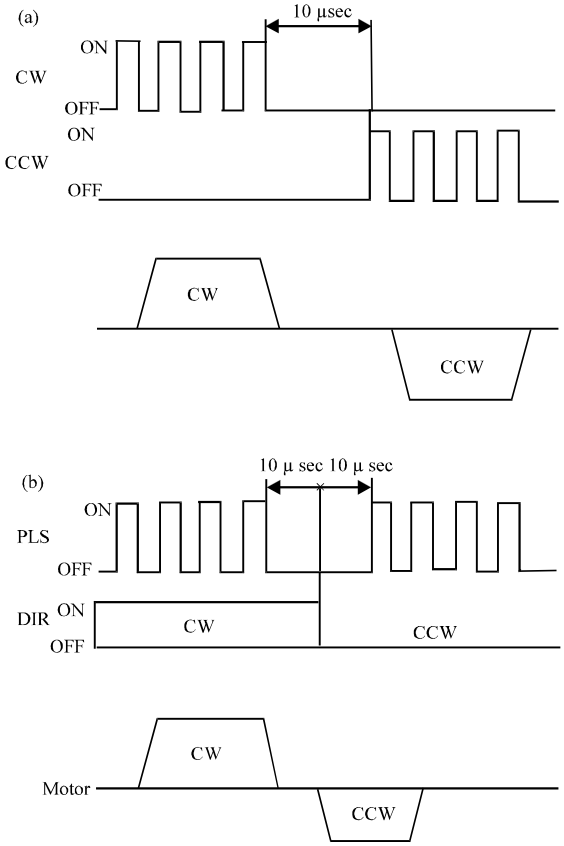

Fig. 8: Two pluse input methods

method. The two-pulse method has CW and CCW inputs as shown in Fig. 8 (a) and the motor rotates according to the input. The one-pulse method also has two inputs, one for pulse input and the other for direction. If the direction input is on then the motor rotates CW and vice versa as shown in Fig. 8 (b).

Table 1: Step angle

SW2	SW3	SW4	Mode	Resolution	Step angle (°)
OFF	OFF	OFF	1	200	1.8
OFF	OFF	ON	2	400	0.9
OFF	ON	OFF	4	800	0.45
OFF	ON	ON	8	1600	0.225
ON	OFF	OFF	16	3200	0.1125

Table 2: Distance for one step angle (µm)

Step angle	1.8	0.9	0.45	0.225	0.1125	Remarks
1 pulse	5	2.5	1.25	0.625	0.31	Eq.(5)
10 pulse	61.8	31.2	15.7	8.09	3.91	2-Pulse method
Avg.	6.18	3.12	1.57	0.81	0.39	2nd row/10
Diff.	-1.18	-0.62	-0.32	-0.19	-0.08	1st row-3rd row

Moving distance per unit pulse: We now calculate the axial moving distance for the step angle. The lead of the ball screw shaft (SG1001) coupled to the stepping motor is 1 mm. The lead is the distance that the nut which is connected to the slider of the Z-axis driver, moves when the screw shaft is rotated once; that is when the stepping motor rotates once, the slider moves 1 mm in the axial direction. Further, if the stepping motor receives a single pulse input, it rotates 1.8°. For this 1.8° rotation, the slider coupled with the stepping motor moves the following distance in the axial direction:

$$\text{Distance/Step angle} = (\text{lead}/360°)\times\text{Step angle} = (1/360°)\times 1.8° = 0.005\ \text{mm} = 5\ \mu\text{m/pulse} \quad (5)$$

From the calculation, the theoretical distances as shown in Table 2 are obtained. It is necessary to

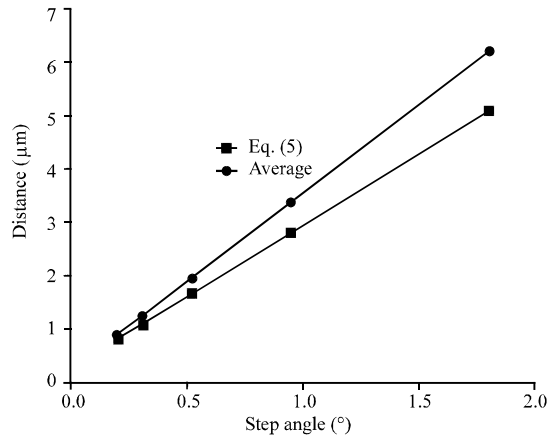

Fig. 9: Measured and calculated distances

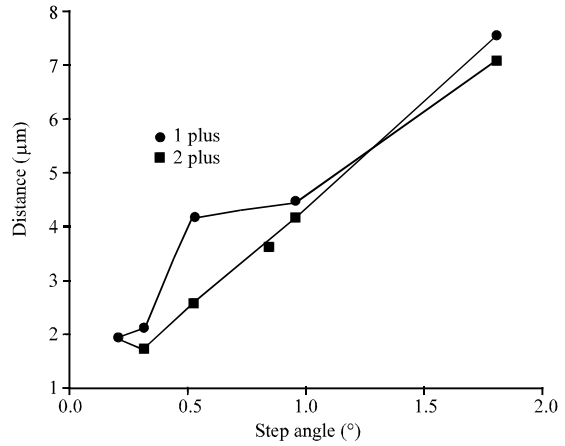

Fig. 10: Accuracy verification by pulse method

Table 3: Differences between maximum and minimum distances for 10 repetitions

Step angle	1.8°	0.9°	0.45°	0.225°	0.1125°
1 pulse	7	4.2	3.9	1.7	1.5
2 pulse	7.5	3.9	2.2	1.3	1.5

determine the correction value required for controlling the device connected to the load by comparing the measured axial movement values at each step angle with these calculated values. The measured and calculated distances are shown in Fig. 9. The difference between the measured and calculated values gradually decreases as the step angle decreases. Especially, it shows 1 μm difference per one pulse at full stepping angle (1.8°). This difference may cause performance deterioration during high precision autofocusing.

Accuracy verification: The first test verified the exactness of the Z-axis test bench distance moved per unit pulse. The test was repeated to verify accuracy. The test results show the difference between the maximum and minimum distances for each step angle. The test was repeated 10 times for each step angle while moving in the forward (CW) and backward directions (CCW).

The difference between the maximum and minimum moving distances is the largest at full step angle (1.8°). As the step angle decreases, the difference between the maximum and minimum values also, decreases gradually by 1-2 μm. As shown in Fig. 10 and Table 3, a step angle with large difference is not suitable for position control of high-precision autofocusing because the large difference causes control in accuracy and malfunction. As a result, it is necessary to use the microstepping range (0.45-0.1125°) which can maintain an accuracy in the range of 1-2 μm for precise position control. However, owing to the nature of the stepping motor, the torque with micro stepping control is reduced by more than 30% compared to full stepping control. Therefore, either full stepping or micro stepping should be applied depending on the load type and torque characteristics. The test results can be used to determine the proper stepping method.

CONCLUSION

In this research, we propose a GUI-based autofocusing system for automatic optical inspection of FPDs. The major components are a Z-axis test bench, MCU and supervising software. A ballscrew shaft which is coupled to the stepping motor, lets the test bench move linearly per pulse received by the stepping motor. Photocouplers are used to determine the motor speed which can be calculated by dividing the time difference by the distance between the two photocouplers. The supervising software is programmed in C# and implemented with user-friendly GUI-based windows. To verify the requirements of high precision inspection we tested the moving distance per pulse for various driving modes and repeated same movement to check the reliability of the test bench. The prototype is well organized and the required precision is met as it moves less than 10 μm. More advanced software functions will be included in the next study and the test bench performance can be improved by modifying the driver setting in future research.

ACKNOWLEDGEMENTS

This research was supported by the sabbatical research grant from Daegu Catholic University in 2018.

REFERENCES

Chun, K., K. Lee, D. Lee and B. Kim, 2018. Analysis of AOI system parameters for FOG image enhancement. Adv. Sci. Lett., 24: 4926-4930.

Chung, M.J., S.Y. Son and Y.H. Yee, 2010. High precision XY stage for production and inspection equipment of organic light-emitting diode display. Adv. Appl. Mech. Eng. Technol., 1: 19-34.

Dong, X.F., Z.Y. Han, S.Y. Liao and X.X. Yi, 2014. Study on semiconductor surface defect detection based on machine Vision. Metrolo. Meas. Technol., 5: 22-24.

Jing, D., X. Peng, Y. Zhijia and M. Ji-Kai, 2015. Micron defect inspection for wafer surface. Comput. Eng. Des., 36: 1671-1675.

Kim, B., D. Lee, K. Lee and K. Chun, 2017. DIC consistent calibration for indentation mark verification in ACF images. J. Eng. Appl. Sci., 12: 6666-6671.

Lee, D., K. Lee, K. Chun and B. Kim, 2018. High definition image acquisition for automatic optical inspection using light sources characteristics. Adv. Sci. Lett., 24: 4936-4941.

Martinez, S.S., J.G. Ortega, J.G. Garcia, A.S. Garcia and E.E. Estevez, 2013. An industrial vision system for surface quality inspection of transparent parts. Intl. J. Adv. Manuf. Technol., 68: 1123-1136.

Tao, X., Z.T. Zhang, F. Zhang, Y. Shi and D. Xu, 2014. Development of detection techniques of surface defects for large aperture optical elements based on machine vision. Proceedings of the 33rd Chinese Conference on Control, July 28-30, 2014, IEEE, Nanjing, China, pp: 2935-2940.

Yubao, L., 2013. Research of surface defects detection algorithm based on machine vision. Master Thesis, Central South University, Changsha, China.